Vertical Structure of Shadow Zone Arrivals: Comparison of Parabolic Equation Simulations and Acoustic Data

10 November 2006 through 30 October 2010

Lora J. Van Uffelen
University of Hawaii at Manoa[1]
Department of Ocean and Resources Engineering
School of Ocean and Earth Science and Technology
1000 Pope Road, MSB 205
Honolulu, HI 96822
phone: (808) 956-3391 email: loravu@hawaii.edu

Award Number: N00014-07-1-0270
Final Technical Report

OBJECTIVES

Observations made on horizontal SOSUS receiving arrays during the Acoustic Thermometry of Ocean Climate (ATOC) experiment in the 1990s show that acoustic energy penetrates significantly deeper in the water column below the lower turning points of the predicted acoustic ray paths than expected from diffraction alone [1]. This energy appears anomalously deep in the water column, but the measured travel times correspond well with timefronts predicted to have cusps several hundred meters above the depth of the receivers.

The primary objective of this effort was to examine the vertical structure of these "shadow-zone arrivals," and to determine the role of oceanic variability in contributing to the vertical scattering. Acoustic vertical line array (VLA) data from the Spice Experiment (SPICEX) were compared with parabolic equation simulations to determine the predictability of the extension of acoustic timefronts into the shadow zone.

APPROACH

In June 2004, two source moorings and a set of hydrophone arrays were deployed in the North Pacific Ocean as part of SPICEX. (SPICEX was one component of the larger 2004 NPAL experiment, which also included the Long-range Ocean Acoustic Propagation EXperiment (LOAPEX) and the Basin Acoustic Seamount Scattering EXperiment (BASSEX).) The two closely spaced VLAs together virtually spanned the full ocean depth, enabling observation of the vertical structure of the timefront arrivals. The two source moorings were located at ranges of 500 km and 1000 km from the VLAs, each

1 Note: All work was completed while Lora Van Uffelen was a graduate student and, subsequently, a postdoc at the Scripps Institution of Oceanography at the University of California San Diego.

supporting acoustic sources at both 750 meters, the approximate depth of the sound channel axis, and 3000 meters, slightly above the surface conjugate depth. Receptions from all four sources were analyzed to determine the level of scattering into the shadow zone.

The focus of prior analysis of long-range propagation data has been acoustic travel time, with less attention paid to the intensity of arrivals; however, absolute intensities are essential to make meaningful comparisons between acoustic receptions and between receptions and simulated data. The VLA receivers were fully calibrated. The intensities of the measured receptions were calculated using the measured hydrophone sensitivity and VLA system gain, taking account of the signal processing gains achieved using large time-bandwidth signals. The predicted intensities of the receptions were calculated using the measured source functions and transmission losses from broadband parabolic equation simulations.

These calibrations enabled direct intensity comparisons of daily incoherent averages of hydrophone data with Monte Carlo parabolic equation simulations incorporating several realizations of stochastic internal-wave fields [2]. Three different environments were considered: a range-dependent profile developed using underway CTD (UCTD) measurements taken at the time of the experimental deployment, the mean sound-speed profile, and a mean sound-speed profile perturbed to stochastically simulate the oceanic sound-speed perturbation due to internal waves [3].

Acoustic ray propagation simulations through a mean, unscattered sound-speed profile were performed to quantitatively define the expected depth of the timefront cusps, i.e., the upper limit of the acoustic shadow zone. The upper turning points of the rays associated with the deep cusps were determined to indicate the depths at which the acoustic rays are most sensitive to scattering due to internal waves [4].

The evolution of monthly incoherent averages of acoustic timefronts from June to November 2004 was investigated to determine the effect of the seasonally dependent upper-ocean sound-speed structure on deep shadow-zone arrivals. Depth-dependent energy profiles of individual lower cusps of monthly incoherent timefront averages were calculated to determine the effect of the seasonally dependent upper-ocean sound-speed structure on deep shadow-zone arrivals. Energy profiles for the same cusps were also calculated for parabolic equation propagation simulations based upon hydrographic measurements taken at the time of the deployment in June 2004 as well as during LOAPEX in September 2004 [5].

Temperature fluctuation data from Seabird MicroCAT (Conductivity And Temperature) sensors affixed to the VLA mooring were compared with the empirical Garrett-Munk internal-wave energy spectrum [6] to determine which energy level (if any) appropriately describes the amount of variability in the region of the SPICEX moorings.

The Philippine Sea is a very different and much more dynamic environment with anticipated high levels of internal wave activity. One objective of the month-long NPAL

Philippine Sea Pilot Experiment conducted in April 2009 is to better understand the time-space scales of ocean variability in the Philippine Sea. Temperature fluctuation data were collected on the Distributed Vertical Line Array (DVLA) mooring from Seabird MicroCAT sensors and temperature recorders, as well as from precision thermistors housed in the hydrophone modules themselves, which were calibrated following the PhilSea09 deployment. These measurements were analyzed to determine whether the internal wave structure could be described using the GM spectrum, as it was in the North Pacific.

RESULTS

Acoustic data received during SPICEX clearly show vertical extension of timefront cusps 500-800 m below depths of lower cusps predicted by deterministic rays propagated through a range-independent sound-speed environment (Figure 1).

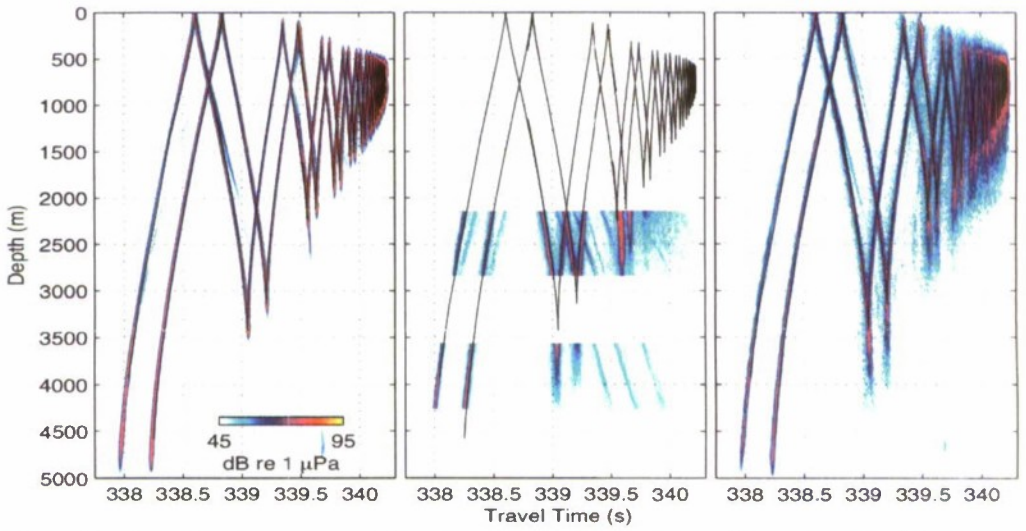

Figure 1: Acoustic ray propagation simulation from an axial source at 500-km range to VLA receivers overlaid on parabolic equation simulation for a range-independent profile (left), a profile including scattering consistent with the Garrett-Munk internal-wave energy spectrum (right), and an incoherent average of acoustic receptions received on the Deep VLA in the month of June 2004 (middle). The incoherent average of the measured receptions has been aligned with the predicted timefront. Three steep arrivals corresponding to rays that reflect from the sea surface and seafloor are clearly evident in the receptions between 339 and 340 seconds, but will not be studied here.

Intensity comparisons demonstrate that parabolic equation simulations incorporating sound-speed fluctuations consistent with the Garrett-Munk internal wave spectrum at full strength (1GM) are adequate to describe the observed structure and extent of measured acoustic shadow-zone arrivals. The comparisons focus on a single day of acoustic transmissions at a time coinciding with the collection of the environmental data that formed the basis for the sound-speed profiles used in the simulations.

The 1000-km propagation path from the axial source to the Deep VLA provides several examples of shadow-zone extensions. The most prominent of these extensions are the second pair of lower turning points, arriving immediately after 675 seconds (Figure 2).

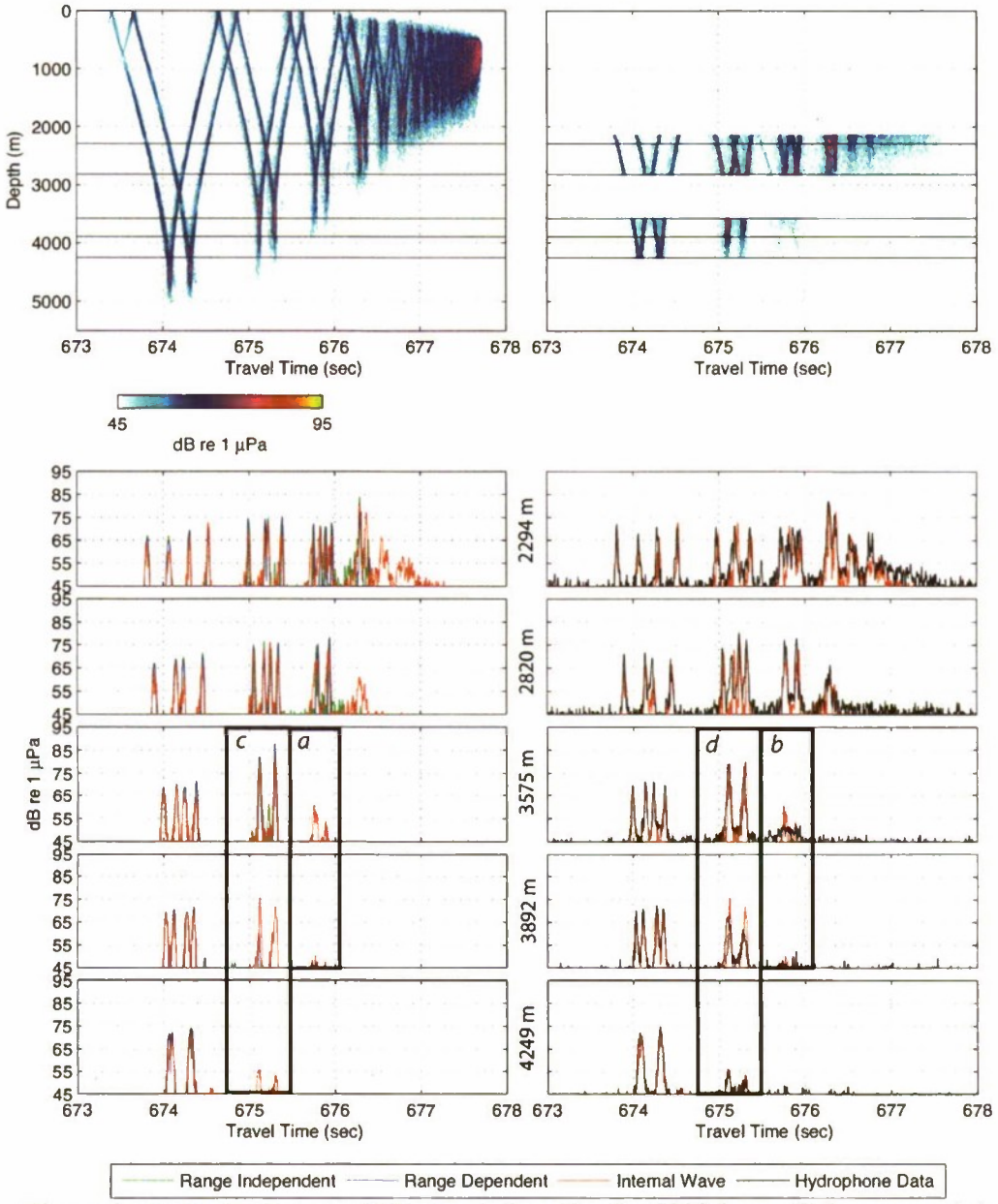

Figure 2: Intensity-averaged PE simulations for the 1000-km path from an axial source to the deep portion of the VLA incorporating five realizations of 1 GM internal wave fields (top left), and an intensity average of six receptions of acoustic data received on yearday 167 (top right). Horizontal black lines indicate depths where slices of the internal wave PE simulation timefront are compared with similar range-dependent and range-independent predictions (lower left) and acoustic hydrophone data (lower right).

The predicted intensities of range-independent, range-dependent and internal wave simulations are consistent at depths above 3575 meters, but only the internal-wave scattered arrival extends past that depth to the deepest hydrophone on the VLA at 4249 meters (Figure 2(c)). Internal-wave simulations compare well with measured intensities at the 3575 and 4249-meter depths, and even over-predict the intensity of the shadow-zone arrival when compared with the hydrophone data at the 3892-meter depth (Figure 2(d)).

A more quantitative measure of the vertical extension of the cusp is the energy profile of the cusp (Figure 3). The upper limit of the shadow zone is located where the energy for the range-independent calculation rapidly decreases. The internal wave simulation appropriately describes the shadow-zone arrivals below both cusps with rms differences from the measured energy levels of 2.5 dB for the first cusp and 4.0 dB for the second cusp.

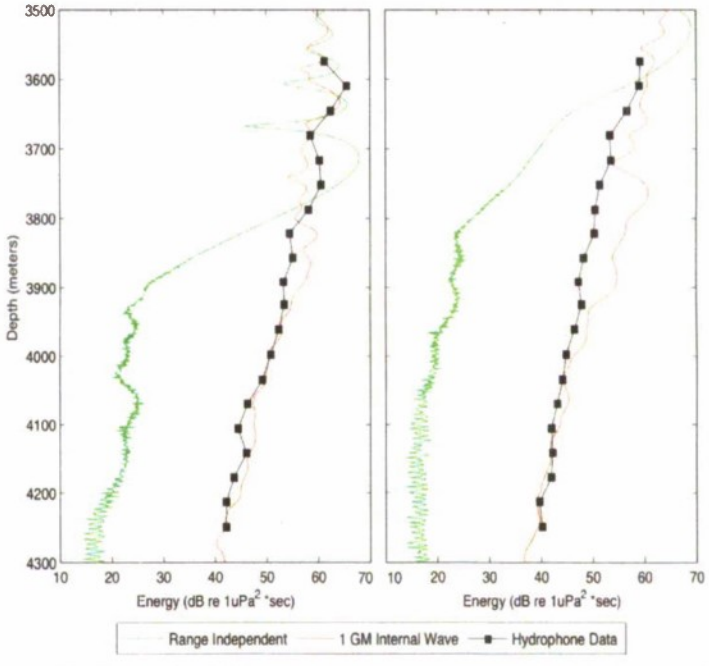

Figure 3: Energy in the pair of lower cusps occurring after 675 seconds for the axial source and a 1000-km propagation path. Energy was calculated for a time window of 675.0 to 675.2 seconds for the first cusp (left) and 675.2 to 675.4 seconds for the second cusp (right). Hydrophone data is shown for the 20 deepest phones on the VLA.

In addition to deep shadow-zone extensions, receptions from off-axis sources reveal scattering back up towards the axis at the end of the arrival pattern, which is not predicted by range-independent models, indicating another type of shadow zone at the end of the arrival pattern (not shown). This scattering occurs predominantly along acoustic timefronts, which is consistent with the observations of scattering for deep shadow-zone arrivals. Parabolic equation simulations incorporating scattering consistent with an

internal-wave energy level of 1 GM appropriately account for the amount of scattering seen both in axial and deep-shadow zone arrivals.

Observations of temperature fluctuation from MicroCAT sensors mounted on the VLA are also consistent with an internal-wave energy level of approximately 1 GM, although instruments located above 200 m indicate higher variability (Figure 4).

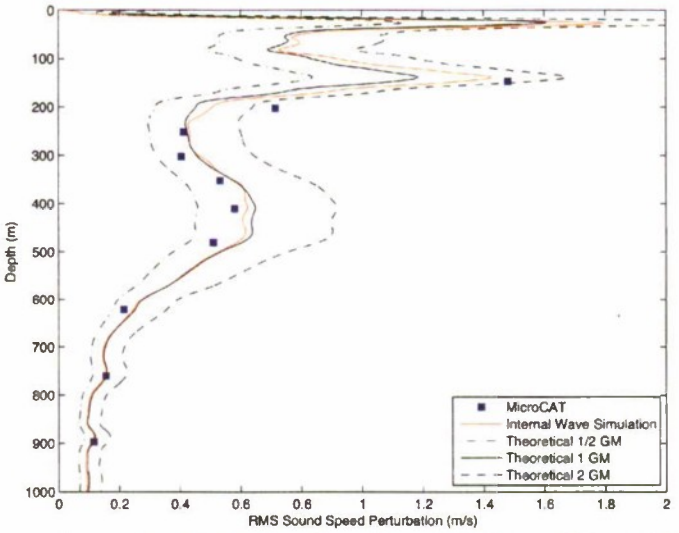

Figure 4: Rms sound-speed perturbation based on data from MicroCAT sensors on the VLA compared with rms sound-speed perturbations generated for 1-GM stochastic internal-wave simulations. Calculated rms sound-speed perturbations based on the theoretical variance of the Garrett-Munk spectrum for energy levels of ½ GM, 1 GM, and 2 GM are also included.

Preliminary fluctuation calculations from Seabird MicroCAT sensors deployed in the PhilSea09 Pilot Study indicate that GM internal-wave energy in the upper ocean is significantly higher than what was observed in the North Pacific during SPICEX.

Incoherent monthly averages of acoustic timefronts demonstrate that the depth of the pair of lower cusps arriving immediately after 339 seconds on Figure 1 increases from June to November and displays dramatic deepening in the month of November. A magnification of the second lower cusp in the pair is shown in Figure 5.

The top panels of Figure 6 show the energy in each of the cusps in this pair as a function of depth. Energy profiles for the monthly timefront averages are compared with energy profiles for unscattered and internal-wave scattered simulations based on both June and September sound-speed environments.

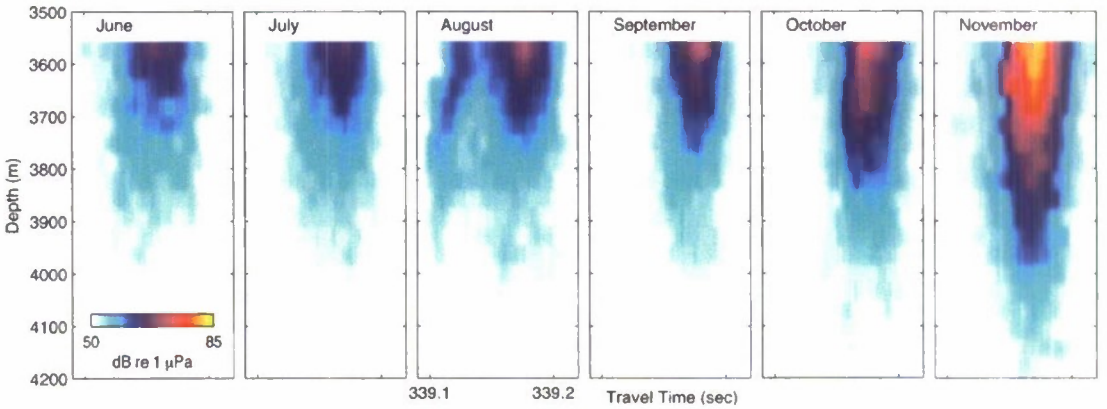

Figure 5: Monthly incoherent average of measured acoustic intensities (dB re 1 μPa) as a function of travel time and hydrophone depth for the second cusp on the 500-km timefront shown in Figure 1.

The unscattered energy profile is characterized by a diffraction pattern culminating in a distinct peak, below which it quickly decays. The energy profiles of the internal-wave simulations do not exhibit this intense peak but have a more scattered profile, which distributes the energy to greater depths. The acoustic data for the months of June through October generally fall between the internal-wave predicted energy profiles for the June and September sound-speed environments, and the month of November is an outlier.

No environmental data are available in the upper ocean at the location of the mooring for the month of November, however, historical data predict that a steep temperature gradient, referred to as the summer thermocline develops from June through September as the surface waters warm and subsides dramatically in November as the surface cools and the heat content of the warm surface waters is distributed to greater depths. The changes in depths of the cusps are likely due to the changing sound-speed profile and are therefore deterministic.

Energy profiles of the first two pairs of cusps on the 1000-km timefront (Figure 2) are also included Figure 6. The lower panels, showing the second pair of cusps, exhibit similar behavior to those in the first pair of cusps on the 500-km timefront, shown in the upper panels, with a dramatic increase in energy in the month of November.

The first pair of cusps on the 1000-km timefront, shown in the middle panels of Figure 6, exhibit very different behavior. The upper phones display the highest energy content in June and the energy level progressively decreases in subsequent months, however the lower phones have the lowest energy in June. June therefore displays the most unscattered profile, with a strong peak that decays quickly, whereas later months, such as November, have more vertical energy profiles, indicating increased scattering. The effect is also present in the internal-wave simulations for June compared with September.

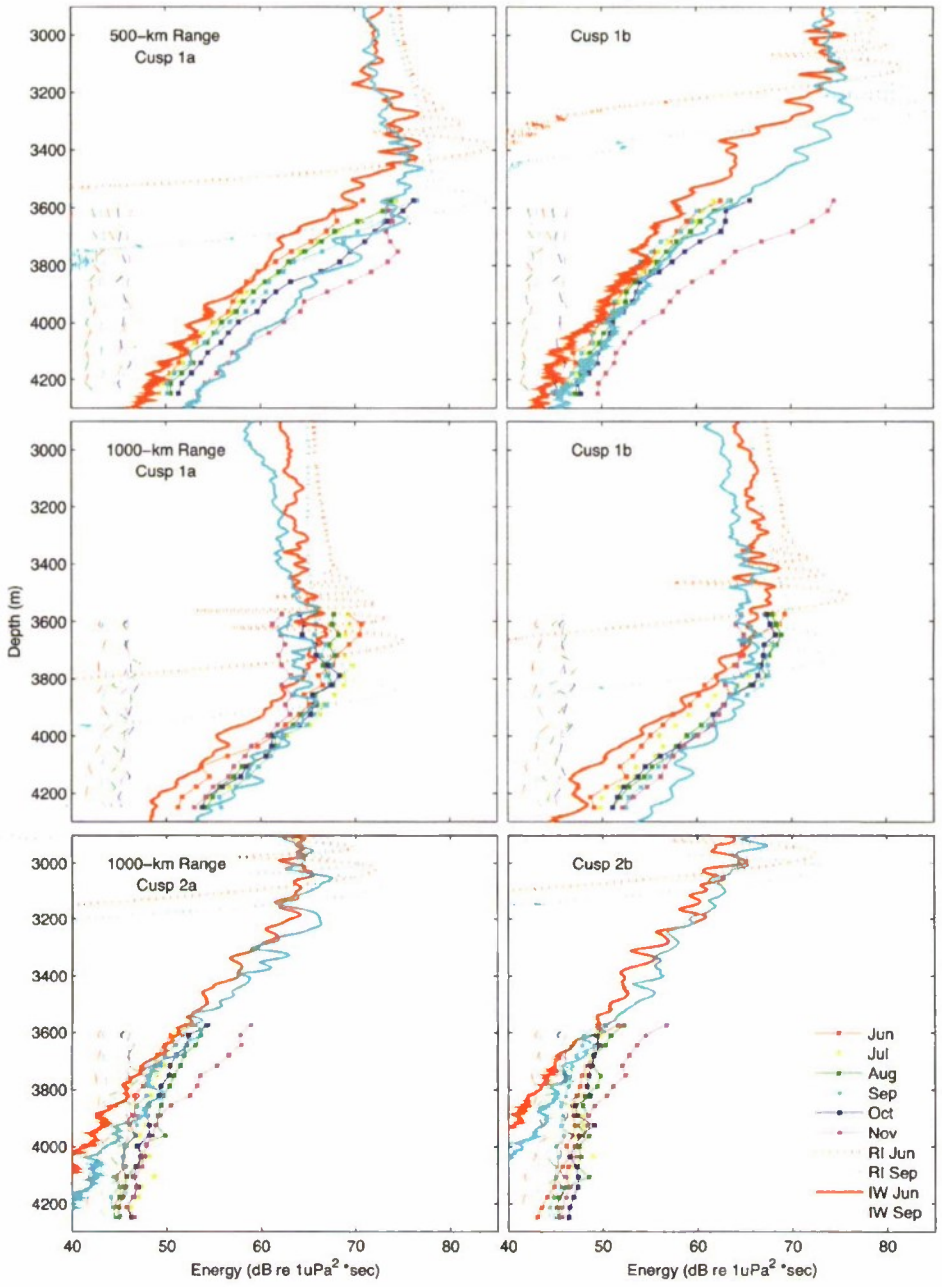

Figure 6: Energy in the first (left) and second (right) cusps in set 1 on the 500-km timefront (top), set 1 on the 1000-km timefront (middle), and set 2 on the 1000-km timefront (bottom). Hydrophone data are shown for June through November for the 20 phones on the lower segment of the DVLA. Noise levels for each month are depicted by dashed lines colored to correspond with the acoustic data. Energy calculated for range-independent and internal-wave PE simulations for both June and September profiles are included.

The difference between this set of lower cusps and the two discussed previously is that the upper turning points for this set of acoustic ray arrivals are shallower (on the order of 20 m for the June profile). The June rays likely demonstrate less scattering by internal-wave fluctuations because they turn very near the sea surface, where internal-wave sound-speed perturbations approach zero. Conversely, in November the rays are likely refracting off the base of the remnant summer thermocline, where gradients are strong and internal-wave variability is high, giving the more scattered profile indicated by slower decay in energy with depth that is observed.

The energy profile of cusps arriving later in the timefront pattern (not shown), resulting from lower-angle rays with deeper upper turning points, display less seasonal dependence than the earlier arrivals with upper turning points in the upper ocean.

The relationship between time of year and shadow-zone extension therefore is not direct. Shadow-zone arrivals refer to energy that arrives below the cusps of unscattered arrivals, so the depth at which an arrival is considered a shadow-zone arrival can change dramatically based on the shape of the sound-speed profile. The depth to which the timefronts extend as the seasons change is a complex combination of deterministic changes in the depths of the lower cusps as the range-average profiles evolve and of the amount of scattering, which depends on the depths of the upper turning points and the mean vertical gradients at those depths.

SUMMARY

Acoustic shadow-zone arrivals were observed 800-1000 m below the depth of predicted timefront cusps in SPICEX data. A new type of shadow zone arrivals, axial-shadow zone arrivals, were discovered in transmissions from deep acoustic sources. Parabolic equation simulations incorporating stochastic sound-speed perturbations consistent with the Garrett-Munk internal wave spectrum at full strength account for the intensity and vertical extent of shadow-zone arrivals at times where environmental observations are available. Observations of sound-speed fluctuations on MicroCAT data during SPICEX indicate an internal wave energy level of approximately 1 GM, although initial observations in the Philippine Sea indicate higher internal wave strength. The depths to which lower timefront cusps extend as the seasons change is a complex combination of deterministic changes in the depths of the lower cusps as the range-average profiles evolve and the amount of scattering, which depends on the depths of the upper turning points of associated rays and the vertical gradients at those depths.

ACKNOWLEDGMENTS

This work was funded as a graduate student traineeship award, and formed the basis of Lora Van Uffelen's Ph.D. dissertation, which she successfully defended on August 24, 2009. Dr. Van Uffelen would like to thank ONR for continual support throughout her graduate and postdoctoral studies. She would also like to acknowledge Peter Worcester, her graduate advisor and postdoctoral mentor, as well as her dissertation advisory committee: Bruce Cornuelle, Daniel Rudnick, Walter Munk and William Kuperman, all

of the Scripps Institution of Oceanography, Kathleen Wage of George Mason University, and William Coles of the electrical engineering department at the University of California, San Diego, as well as collaborators Matthew Dzieciuch of the Scripps Institution of Oceanography and John Colosi at the Naval Postgraduate School.

PUBLICATIONS

Van Uffelen, L. J., P. F. Worcester, M. A. Dzieciuch, D. L. Rudnick, and J. A. Colosi (2010), "Effects of upper ocean sound-speed structure on deep acoustic shadow-zone arrivals at 500- and 1000-km range." J. Acoust. Soc. Am., 127, 2169-2181.

Van Uffelen, L. J., P. F. Worcester, M. A. Dzieciuch, and D. L. Rudnick (2009), "The vertical structure of shadow-zone arrivals at long range in the ocean." J. Acoust. Soc. Am. 125, 3569-3588.

Stephen, R. A., S. T. Bolmer, I. Udovydchenkov, P. F. Worcester, M. A. Dzieciuch, L. J. Van Uffelen, J.A. Mercer, R. K. Andrew, L. J. Buck, J. A. Colosi, B. M. Howe (2008), "NPAL04 OBS Data Analysis Part 1: Kinematics of Deep Seafloor Arrivals." Woods Hole Oceanographic Institution Technical Report WHOI-2008-03.

PUBLISHED ABSTRACTS

Van Uffelen, L. J., K.E. Wage (2010), "Ocean acoustic tomography: Live from the Philippine Sea."J. Acoust. Soc. Am., 127, 1913. Presented remotely from onboard the R/V Roger Revelle at the April 2010 Meeting of Acoustical Society of America in Baltimore, MD. **Invited Paper**.

Van Uffelen, L. J., P. F. Worcester (2009), "Characterization of deep acoustic shadow-zone arrivals."J. Acoust. Soc. Am., 126, 2159. Presented at October 2009 Meeting of Acoustical Society of America in San Antonio, TX. **Student Paper Award in Acoustical Oceanography.**

Van Uffelen, L. J., P. F. Worcester, M. A. Dzieciuch (2008), "Absolute Intensities of Acoustic Shadow-Zone Arrivals." J. Acoust. Soc. Am., 123, 3464. Presented at Acoustics '08 Conference in Paris, France, July 2008.

Van Uffelen, L. J., P. F. Worcester, M. A. Dzieciuch, and D. L. Rudnick (2006), "Mixed Layer Effects on Acoustic Arrival Structure." J. Acoust. Soc. Am., 120, 3021. Presented at December 2006 Meeting of Acoustical Society of America in Honolulu, HI.

REFERENCES

[1] Dushaw, B.D., Howe, B.M., Mercer, J.A., Spindel, R.C., and The ATOC Group (A. B. Baggeroer, T. G. Birdsall, C. Clark, J. A. Colosi, B. D. Cornuelle, D. Costa, B. D. Dushaw, M. A. Dzieciuch, A. M. G. Forbes, B. M. Howe, D. Menemenlis, J. A. Mercer, K. Metzger, W. H. Munk, R. C. Spindel, P. F. Worcester, and C. Wunsch) (1999).

"Multimegameter-Range Acoustic Data Obtained by Bottom-Mounted Hydrophone Arrays for Measurement of Ocean Temperature," IEEE J. Ocean. Eng. **24**, 202-214.

[2] Collins, M.D. (1989). "A higher-order parabolic equation method for wave propagation in an ocean overlying an elastic bottom," J. Acoust. Soc. Am. **86**, 1459-1464.

[3] Colosi, J.A., Brown, M.G. (1998). "Efficient numerical simulation of stochastic internal-wave-induced sound-speed perturbation fields," J. Acoust. Soc. Am. **103**, 2232-2235.

[4] Flatté, S.M., Dashen, R., Munk, W.H., Watson, K.M., and Zachariasen, F. (1979). *Sound transmission throuh a fluctuation ocean.* Cambridge University Press, New York.

[5] Mercer, J.A., Colosi, J.A., Howe, B.M., Dzieciuch, M.A., Stephen R., and Worcester. P.F. (2009). "The Long-range Ocean Acoustic Propagation Experiment," IEEE J. Ocean. Eng. **34**, 1-11.

[6] Garrett, C., and Munk, W. (1979). "Internal waves in the ocean," Ann. Rev. Fluid Mech. **11**, 339-369.

REPORT DOCUMENTATION PAGE	Form Approved OMB No. 0704-0188

1. REPORT DATE (DD-MM-YYYY)	2. REPORT TYPE	3. DATES COVERED (From - To)
02-22-2011	Final Technical Report	10 NOV 2006 - 30 OCT 2010

4. TITLE AND SUBTITLE
ONR Graduate Traineeship Award in Ocean Acoustics: Vertical Structure of Shadow Zone Arrivals

5a. CONTRACT NUMBER

5b. GRANT NUMBER
N00014-07-1-0270

5c. PROGRAM ELEMENT NUMBER

6. AUTHOR(S)
Lora Van Uffelen

5d. PROJECT NUMBER

5e. TASK NUMBER

5f. WORK UNIT NUMBER

7. PERFORMING ORGANIZATION NAME(S) AND ADDRESS(ES)
The Regents of the University of California San Diego: UCSD
Office of Contract and Grant Administration
9500 Gilman Drive
La Jolla, CA 92093-0210

8. PERFORMING ORGANIZATION REPORT NUMBER

9. SPONSORING/MONITORING AGENCY NAME(S) AND ADDRESS(ES)
Office of Naval Research
875 North Randolph Street
Arlington, VA 22203-1995

10. SPONSOR/MONITOR'S ACRONYM(S)

11. SPONSOR/MONITOR'S REPORT NUMBER(S)

12. DISTRIBUTION/AVAILABILITY STATEMENT
Approved for public release; distribution is unlimited

13. SUPPLEMENTARY NOTES

14. ABSTRACT

Acoustic shadow-zone arrivals were observed 800-1000 m below the depth of predicted timefront cusps in SPICEX data. A new type of shadow zone arrivals, axial-shadow zone arrivals, were discovered in transmissions from deep acoustic sources. Parabolic equipment simulations incorporating stochastic sound-speed perturbations consistent with the Garrett-Munk internal wave spectrum at full strength account for the intensity and vertical extent of shadow-zone arrivals at times where environmental observations are available. Observations of sound-speed fluctuations on MicroCAT data during SPICEX indicate an internal wave energy level of approximately 1 GM, although initial observations in the Philippine Sea indicate higher internal wave strength. The depths to which lower timefront cusps extent as the seasons change is a complex combination of deterministic changes in the depths of the lower cusps as the range-average profiles evole and the amount of scattering, which depends on the depths of the upper turning points of associated rays and the vertical gradients at those depths.

15. SUBJECT TERMS

16. SECURITY CLASSIFICATION OF:			17. LIMITATION OF ABSTRACT	18. NUMBER OF PAGES	19a. NAME OF RESPONSIBLE PERSON
a. REPORT	b. ABSTRACT	c. THIS PAGE			Lora Van Uffelen
unclassified	unclassified	unclassified	unlimited	11	19b. TELEPHONE NUMBER (Include area code) 858-534-4453